Available online at www.sciencedirect.com
ScienceDirect
Pattern Recognition 40 (2007) 3209–3224
PATTERN RECOGNITION
THE JOURNAL OF THE PATTERN RECOGNITION SOCIETY
www.elsevier.com/locate/pr

Face and palmprint pixel level fusion and Kernel DCV-RBF classifier for small sample biometric recognition

Xiao-Yuan Jing[a,*], Yong-Fang Yao[a], David Zhang[b], Jing-Yu Yang[c], Miao Li[d]

[a]*Institute of Automation, Nanjing University of Posts and Telecommunications, Guangdong Road No. 38, Nanjing 210003, China*
[b]*Department of Computing, Hong Kong Polytechnic University, Kowloon, Hong Kong*
[c]*Institute of Computer Science, Nanjing University of Science and Technology, Nanjing, China*
[d]*Institute of Computer Science, Harbin Institute of Technology, Harbin, China*

Received 13 April 2006; received in revised form 19 January 2007; accepted 22 January 2007

Abstract

Recently, multi-modal biometric fusion techniques have attracted increasing attention and interest among researchers, in the hope that the supplementary information between different biometrics might improve the recognition performance in some difficult biometric problems. The small sample biometric recognition problem is such a research difficulty in real-world applications. So far, most research work on fusion techniques has been done at the highest fusion level, i.e. the decision level. In this paper, we propose a novel fusion approach at the lowest level, i.e. the image pixel level. We first combine two kinds of biometrics: the face feature, which is a representative of contactless biometric, and the palmprint feature, which is a typical contacting biometric. We perform the Gabor transform on face and palmprint images and combine them at the pixel level. The correlation analysis shows that there is very small correlation between their normalized Gabor-transformed images. This paper also presents a novel classifier, KDCV-RBF, to classify the fused biometric images. It extracts the image discriminative features using a Kernel discriminative common vectors (KDCV) approach and classifies the features by using the radial base function (RBF) network. As the test data, we take two largest public face databases (AR and FERET) and a large palmprint database. The experimental results demonstrate that the proposed biometric fusion recognition approach is a rather effective solution for the small sample recognition problem.

Keywords: Multi-modal biometric; Small sample biometric recognition; Face and palmprint; Pixel level fusion; Gabor transform; Kernel discriminative common vectors (KDCV); Radial base function (RBF) network; KDCV-RBF classifier

1. Introduction

Biometric, which refers to the automatic recognition of people based on distinctive physical characteristics (e.g., face, fingerprint, iris, palmprint, signature, gait, etc.), is a topic of considerable current research interest given the growing need for secure transaction processing using reliable methods [1]. Biometric recognition techniques can overcome some of the limitations of traditional personal identification technologies but new algorithms and solutions are still required [2,3]. There are three common difficulties when using biometric data in real-world biometric recognition systems [1]: first, it is often necessary to recognize or identify one individual from among many. More specifically, given an input biometric sample, a biometric system must determine if the pattern is associated with any of a large number of enrolled identities. Second, there is the problem of high dimensionality. Biometric data are usually represented as an image but the high dimensionality of biometric data makes direct classification in image space almost impossible, both because the similarity calculation is computationally very expensive and because it make very large storage demands and so requires a dimension reduction technique prior to recognition. Third, there is the small sample size recognition problem [4–6] which arises because, unlike in optical character recognition problems, large-scale biometric systems make use of a very limited number of training samples.

In real-world applications, it is often difficult to get a satisfactory recognition performance with techniques that use only single-mode biometric. Recently, multi-modal biometric fusion

* Corresponding author. Tel./fax: +86 25 85899381.
E-mail address: jingxy_2000@yahoo.com (X.-Y. Jing).

0031-3203/$30.00
doi:10.1016/j.patcog.2007.01.034

techniques have attracted increasing research interest in the belief that the supplementary information between different biometrics might improve the recognition performance. Hong et al. [7] achieved improvements by integrating fingerprint and face biometric while Jain et al. [8] combined three biometrics: face, fingerprint, and hand geometry. The biometric fusion procedure usually involves two steps. The first is to select an appropriate biometric, one which is able to provide the supplementary information for use in recognition. The second is to design an effective method for fusing the biometric. Broadly, there are three levels of fusion: pixel level, feature level, and decision (or classifier) level [9]. To data, most research on fusion has been done at the highest level, that is, the decision level [10–13].

In this paper, we propose a novel fusion approach that operates at the lowest level, i.e. the pixel level. We use two kinds of biometric: the face feature, which is a representative of contactless biometric (e.g., face, gait [14], ear [15]); and the palmprint feature, which is one of the contacting biometrics (e.g., fingerprint, iris [16], palmprint [17]). The simplest pixel level fusion method is to directly combine the original face and palmprint images, however, so as to acquire more image information for use in small sample biometric recognition, we combine the Gabor-based face and palmprint images. The Gabor transform is a windowed Fourier transform, which is suitable for analyzing gradually changing signals. Face and palmprint images may be regarded as these kinds of signals. The Gabor transform models rather well the receptive field profiles of the cortical simple cells. It has the properties of multi-scale and multi-directional filtering. These properties are in accordance with the characteristics of human vision. Some researchers used the Gabor filtered images for face recognition [18,19]. Kong et al. [17,20] extracted palmprint features using two-dimensional Gabor filters. Therefore, the Gabor transform is suitable for face and palmprint biometric. We demonstrate that there is very small correlation between their normalized Gabor-transformed images.

The fused image data used in real-world applications are usually high-dimensional and large-scale and must be processed using an effective classifier. The classifier should extract appropriate features and use an appropriate classification method. Discrimination analysis techniques are suitable for processing biometric images because they allow the extraction of image discriminative features, reduce dimensionality, and consume less computing time [21]. Two classical linear discrimination techniques are the principal component analysis (PCA) and the linear discrimination analysis (LDA). They have been used to develop many linear and nonlinear discrimination methods such as the Eigenface method [22], the Fisherface method [23], the direct LDA (DLDA) method [24], the uncorrelated optimal discrimination vector (UODV) method [25,41], the discriminant fractional Fourier method [42], the discriminant DCT method [43], the Kernel PCA method [26] and the generalized Kernel discriminant analysis method [27]. One newly developed discrimination method [28] that has been shown to be more effective than some conventional methods, including Eigenface, Fisherface and DLDA, is the discriminative common vectors (DCV) algorithm. In this paper, we extend DCV to the Kernel space and present a new nonlinear discriminative feature extraction approach, the Kernel DCV (KDCV) approach.

The classifier should also use an appropriate feature classification method. Many linear and nonlinear discrimination algorithms use the nearest neighbor (NN) method. For example, the DCV algorithm uses it by employing the Euclidean distance. One of most widely applied neural networks is the radial basis function (RBF) network, which is applied to the function approximation and pattern classification [29–31]. RBF network has four advantages [32,33]: (i) global optimal approximation characteristic, (ii) favorable classification capability, (iii) rapid convergence of learning procedure, and (iv) an optimal network that can accomplish the mapping function in the feed-forward neural networks. In this paper, we demonstrate that the RBF network is more suitable for classifying the KDCV features than the NN method and present a novel classifier, KDCV–RBF, which uses the same kernel function for both KDCV and RBF. The Kernel discrimination methods often adopt the polynomial and Gaussian kernel functions. RBF network generally uses three radial basis functions: the multi-quadric equation, the inverse multi-quadric equation, and Gaussian basis functions [34]. The KDCV–RBF classifier uses the Gaussian function.

We use two largest public face databases (the AR and FERET databases) and a large palmprint database as the test data. The experimental results will show that the proposed fusion approach significantly improves the recognition performance of the small sample biometric problem. The rest of the paper is organized as follows. In Section 2, we describe the Gabor-based pixel level fusion procedure. In Section 3 we describe the KDCV–RBF classifier. In Section 4 we provide the experimental results. Finally, we give the conclusion in Section 5.

2. Gabor-based pixel level fusion

In this section we describe the face and palmprint pixel fusion procedure which is based on Gabor transform.

2.1. Face and palmprint Gabor transform

As an image analysis tool, the Gabor transform is suitable for analyzing gradually changing data such as the face, iris and palmprint images. The circular Gabor filter used here has the following general form:

$$G(x, y, \theta, u, \sigma) = \frac{1}{2\pi\sigma^2} \exp\left\{-\frac{x^2+y^2}{2\sigma^2}\right\} \times \exp\{2\pi \mathrm{i}(ux\cos\theta + uy\sin\theta)\}, \quad (1)$$

where $\mathrm{i}=\sqrt{-1}$, u is the frequency of the sinusoidal wave, θ controls the orientation of the function and σ is the standard deviation of the Gaussian envelope. Fig. 1 shows the face demonstration images of the Gabor transform: (a) shows an original face image; and (b) shows the results of Gabor filtering (expressed by magnitude values). The size of the face image is 60×60. For the filter parameters in Formula (1), σ is set as $\{2, 4, 8, 16\}$, $u = 1/\sigma$ and θ is set as $\{0, 1, 2, 3, 4, 5, 6, 7\} \times (\pi/8)$. So the Gabor transform used in this paper contains four scales and eight orientations.

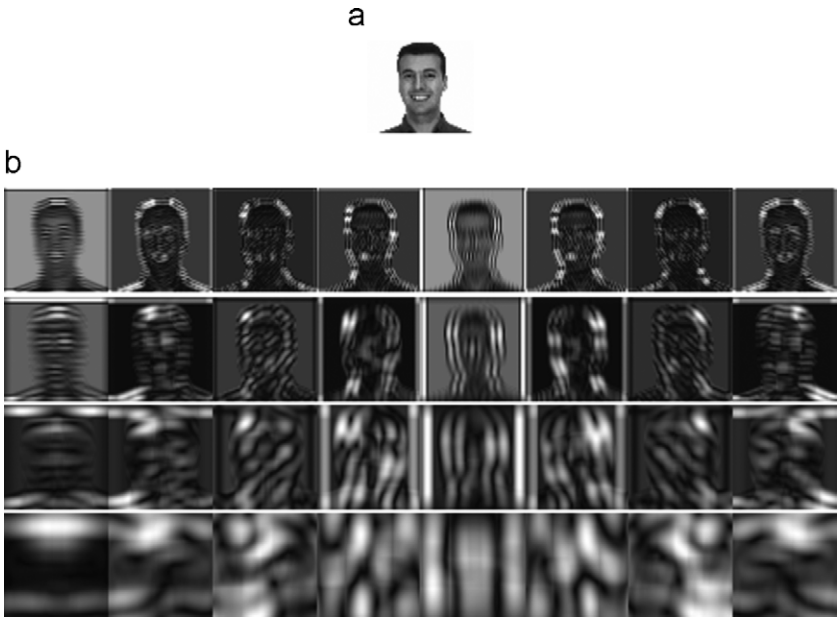

Fig. 1. Face demonstration images of Gabor transform.

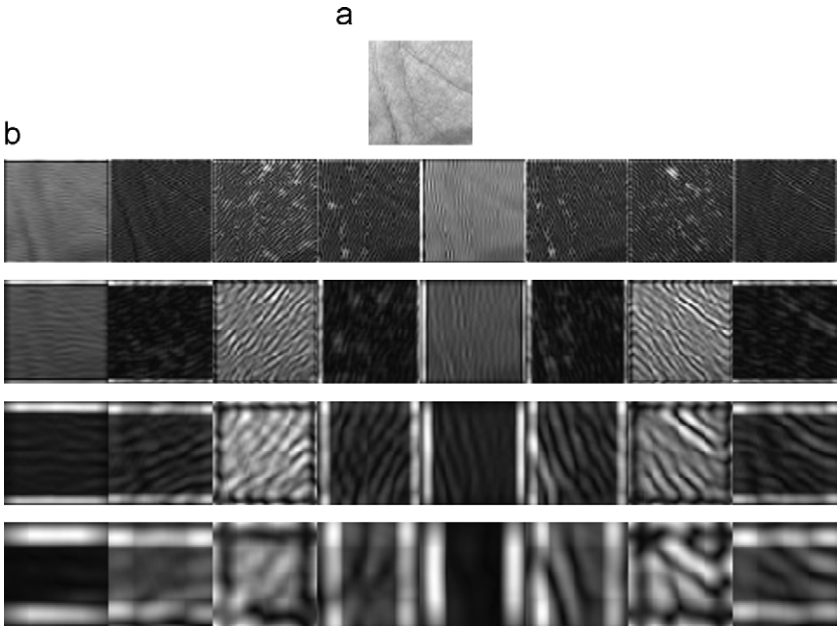

Fig. 2. Palmprint demonstration images of Gabor transform.

Fig. 2 shows the palmprint demonstration images of the Gabor transform: (a) shows an original palmprint image; and (b) shows the results of Gabor filtering (expressed by magnitude values). The size of the original palmprint image is again 60×60.

2.2. Fusion and pixel normalization

We implement the pixel level fusion as follows:

(i) Let X_{face} and X_{palm} separately represent the face and palmprint image sample sets. Assume that x_{face} represents a sample of X_{face} with size 60×60. Performing the Gabor transform on x_{face}, we obtain 32 ($=4 \times 8$) transformed images, as shown in Fig. 1. Combining them, we get a Gaborface image sample $x_{Gaborface}$, the initial size of which is 240×480. To reduce the computational cost, we downsample each transformed image by a ratio equal to 4. So the size of $x_{Gaborface}$ is reduced to 60×120. Similarly, for a sample y_{face} in X_{palm}, we obtain its Gabor-transformed sample $x_{Gaborpalm}$.

(ii) Combining $x_{Gaborface}$ and its corresponding $x_{Gaborpalm}$ vertically, we get a fused image sample x_{fuse}, the size of which is 120×120. Fig. 3 shows a sample fused image

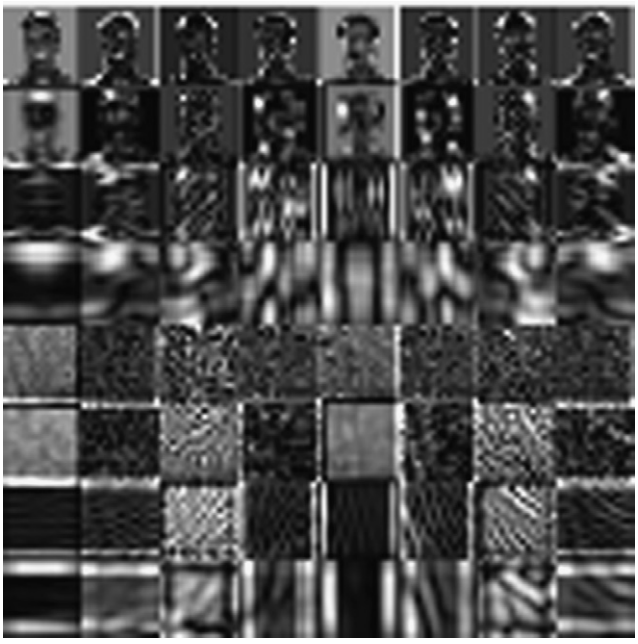

Fig. 3. Sample fused image.

which combines the Gabor-transformed images shown in Figs. 1 and 2. We thus obtain a fused image sample set X_{fuse}.

The imaging conditions of the face and palmprint images are different. For example, they were obtained under different illumination conditions and camera focus settings. Therefore, it is necessary to perform the pixel normalization for fused images. We normalize x_{fuse} as follows:

$$x_{norm\text{-}fuse} = \frac{x_{fuse} - \mu_{fuse}}{\sigma_{fuse}}, \tag{2}$$

where μ_{fuse} and σ_{fuse} indicate the mean value and variance value of X_{fuse}. We thus obtain a normalized sample set $X_{norm\text{-}fuse}$.

2.3. Correlation analysis of pixel level

Let a and b separately express the face and palmprint image parts of $x_{norm\text{-}fuse}$. We use the following formula to evaluate their correlation coefficient $corr(a, b)$:

$$corr(a,b) = \frac{\sum_{i=1}^{60}\sum_{j=1}^{120}|(a_{ij}-\bar{a})(b_{ij}-\bar{b})|}{\left(\left[\sum_{i=1}^{60}\sum_{j=1}^{120}(a_{ij}-\bar{a})^2\right]\times\left[\sum_{i=1}^{60}\sum_{j=1}^{120}(b_{ij}-\bar{b})^2\right]\right)^{1/2}}, \tag{3}$$

where $||$ indicates the absolute value, $\bar{a}$ and $\bar{b}$ are the mean values of a and b. We compute the correlation coefficients of all samples in $X_{norm\text{-}fuse}$, and then obtain the average correlation coefficient $corr(X_{norm\text{-}fuse})$. Table 1 provides the correlation analysis of the face and palmprint images. For the original image sets X_{face} and X_{palm}, we use the same method to calculate their correlation coefficients as $X_{norm\text{-}fuse}$. Table 1 shows that the pixel level correlation of the face and palmprint images is quite small, especially for normalized Gabor-transformed images. This test shows that the Gabor transform is helpful in reducing the correlation between different biometric images.

Table 1
Correlation analysis of the face and palmprint images

Sample sets	Face and palmprint databases combination	Average correlation coefficients
Normalized Gabor-transformed image sample set $X_{norm\text{-}fuse}$	AR and palmprint	0.0344
	FERET and palmprint	0.0395
Original image sample sets X_{face} and X_{palm}	AR and palmprint	0.1351
	FERET and palmprint	0.1185

3. KDCV–RBF classifier

In this section, we describe the KDCV approach and present the KDCV–RBF classifier.

3.1. Nonlinear discrimination analysis in Kernel space

The nonlinear discrimination analysis technique is based on a conceptual transformation from an input space into a nonlinear high-dimensional feature space. For a given nonlinear mapping function Φ, the input data space R^n can be mapped into a feature space F:

$$\Phi : \Re^n \to F, x \mapsto \Phi(x). \tag{4}$$

Correspondingly, a pattern in the original input space $\Re^n$ is mapped into a potentially higher dimensional feature vector in F. Suppose that there are c known pattern classes in the sample set X, l_i is the training sample number of the ith class, and there will be a total of $M = \sum_{i=1}^{c} l_i$ training samples. Let S_W^Φ, S_B^Φ and S_T^Φ separately represent the within-class scatter matrix, the between-class scatter matrix and the total-class scatter matrix in the Kernel space F. They are defined as

$$S_B^\Phi = \frac{1}{M}\sum_{i=1}^{c} l_i(\mu_i^\Phi - \mu^\Phi)(\mu_i^\Phi - \mu^\Phi)^{\mathrm{T}}, \tag{5}$$

$$S_W^\Phi = \frac{1}{M}\sum_{i=1}^{c}\sum_{m=1}^{l_i}(\Phi(x_m^i) - \mu_i^\Phi)(\Phi(x_m^i) - \mu_i^\Phi)^{\mathrm{T}}, \tag{6}$$

$$S_T^\Phi = \frac{1}{M}\sum_{j=1}^{M}(\Phi(x_j) - \mu^\Phi)(\Phi(x_j) - \mu^\Phi)^{\mathrm{T}}, \tag{7}$$

where $\Phi(x_m^i)$ is the mth training sample of the ith class, μ_i^Φ is the mean value of the ith class samples, μ^Φ is the mean value of all training samples, and $\Phi(x_j)$ denotes a training sample

of X. Define the Fisher discriminant criterion in F as

$$J_1(\varphi) = \frac{\varphi^{\mathrm{T}} S_B^{\Phi} \varphi}{\varphi^{\mathrm{T}} S_W^{\Phi} \varphi}, \tag{8}$$

or

$$J_2(\varphi) = \frac{\varphi^{\mathrm{T}} S_B^{\Phi} \varphi}{\varphi^{\mathrm{T}} S_T^{\Phi} \varphi}. \tag{9}$$

The optimal discriminant vector φ is the eigenvector satisfies equations $S_B^{\Phi}\varphi = \lambda S_W^{\Phi}\varphi$ or $S_B^{\Phi}\varphi = \lambda S_T^{\Phi}\varphi$. φ can be expressed by a linear combination of the observations in the Kernel space F, we have

$$\varphi = \sum_{j=1}^{M} a_j \Phi(x_j) = H\alpha, \tag{10}$$

where $H = [\Phi(x_1), \Phi(x_2), \ldots, \Phi(x_M)]$ and $\alpha = (a_1, a_2, \ldots, a_M)^{\mathrm{T}}$. Substituting Eq. (10) into Eqs. (8)–(9), we obtain [27,36]:

$$J_1^{\Phi}(\alpha) = \frac{\alpha^{\mathrm{T}}(KUK)\alpha}{\alpha^{\mathrm{T}}(K(I_N - U)K)\alpha}, \tag{11}$$

and

$$J_2^{\Phi}(\alpha) = \frac{\alpha^{\mathrm{T}}(KUK)\alpha}{\alpha^{\mathrm{T}}(KK)\alpha}, \tag{12}$$

where K is an $M \times M$ kernel symmetric matrix, $K = (K_{ij})_{i,j=1,2,\ldots,M}$, $K_{ij} = \Phi(x_i)^{\mathrm{T}}\Phi(x_j)$; I_N is a $M \times M$ identity matrix; and U is an $M \times M$ block diagonal matrix. $U = \mathrm{diag}(U_1, \ldots, U_c)$ where U_i $(i = 1, 2, \ldots, c)$ is a $l_i \times l_i$ matrix, the elements of which are equal to $1/l_i$. Let $S'_B = KUK$, $S'_W = K(I_N - U)K$ and $S'_T = KK$. Thus, we obtain the basic expressions of the nonlinear discrimination analysis in the Kernel space F.

3.2. KDCV-based feature extraction

The principle of the DCV algorithm is to acquire the optimal projection transform W in the null space of S_W [28]:

$$J(W) = \arg\max_{|W^{\mathrm{T}} S_W W| = 0} |W^{\mathrm{T}} S_B W| = \arg\max_{|W^{\mathrm{T}} S_W W| = 0} |W^{\mathrm{T}} S_T W|, \tag{13}$$

where S_W, S_B and S_T are the within-class, between-class and total scatter matrices in the original feature space. Generally, there are two steps in realizing the DCV algorithm. The first is to obtain the null space of S_W and the common vectors constructing S_T. The second is to get the projection transform W and the DCV. Referring to the DCV algorithm, we realize the KDCV-based feature extraction approach as follows:

(i) Compute the common vectors.
S'_W is an $M \times M$ symmetric matrix. Let R^d be the original sample space, V be the nonnull space of S'_W, and $V^{\perp}$ be the null space of S'_W. We have

$$V = span\{\beta_k | S'_W \beta_k \neq 0, k = 1, 2, \ldots, r\}, \tag{14}$$

and

$$V^{\perp} = span\{\beta_k | S'_W \beta_k = 0, k = r+1, r+2, \ldots, M\}, \tag{15}$$

where r is the rank of S'_W. Let $Q = \{\beta_1, \beta_2, \ldots, \beta_r\}$ and $\bar{Q} = \{\beta_{r+1}, \beta_{r+2}, \ldots, \beta_M\}$. Since $R^d = V \oplus V^{\perp}$, each sample $\Phi(x_m^i) \in R^d$ has a unique decomposition of the form

$$\Phi(x_m^i) = \Phi(y_m^i) + \Phi(z_m^i), \tag{16}$$

where $\Phi(y_m^i) = P\Phi(x_m^i) = QQ^{\mathrm{T}}\Phi(x_m^i) \in V$, $\Phi(z_m^i) = \bar{P}\Phi(x_m^i) = \bar{Q}\bar{Q}^{\mathrm{T}}\Phi(x_m^i) \in V^{\perp}$, and P and $\bar{P}$ are the orthogonal projection operators onto V and $V^{\perp}$, respectively. V can be realized by an eigenanalysis of S'_W. $\{\beta_1, \beta_2, \ldots, \beta_r\}$ are the eigenvectors corresponding to the nonzero eigenvalues of S'_W.
$\Phi(y_m^i)$ and $\Phi(z_m^i)$ separately represent the difference vector and common vector parts of $\Phi(x_m^i)$. It has been proved by Gulmezoglu et al. [35] that for all samples of the ith class, their common vector parts are same. In other words, all of $\Phi(z_m^i)$ $(m = 1, 2, \ldots, l_i)$ are same. We use $\Phi(x_{com}^i)$ to represent the common vector of the ith class instead of $\Phi(z_m^i)$. We rewrite Eq. (16) and calculate $\Phi(x_{com}^i)$ as

$$\Phi(x_{com}^i) = \Phi(x_m^i) - \Phi(y_m^i) = \Phi(x_m^i) - QQ^{\mathrm{T}}\Phi(x_m^i). \tag{17}$$

Thus, we obtain a common vectors set $A = \{\Phi(x_{com}^1), \Phi(x_{com}^2), \ldots, \Phi(x_{com}^c)\}$.

(ii) Compute the optimal projection transform.
Let S_{com}^{Φ} denote the total scatter matrix of A:

$$S_{com}^{\Phi} = \sum_{i=1}^{c} (\Phi(x_{com}^i) - \mu_{com}^{\Phi})(\Phi(x_{com}^i) - \mu_{com}^{\Phi})^{\mathrm{T}}, \tag{18}$$

where

$$\mu_{com}^{\Phi} = \frac{1}{c}\sum_{i=1}^{c} \Phi(x_{com}^i). \tag{19}$$

The optimal projection transform W maximizes

$$J(W) = \arg\max_{|W^{\mathrm{T}} S'_W W| = 0} |W^{\mathrm{T}} S'_T W| = \arg\max_{|W^{\mathrm{T}} S'_W W| = 0} |W^{\mathrm{T}} S_{com}^{\Phi} W|. \tag{20}$$

W is composed of the eigenvectors corresponding to the nonzero eigenvalues of S_{com}^{Φ}. Generally, all classes are independent in the sample set X. Hence, all common vectors are independent and the rank of S_{com}^{Φ} is $c - 1$. We obtain the nonlinear DCV

$$y_i = W^{\mathrm{T}}\Phi(x_{com}^i), \quad i = 1, 2, \ldots, c. \tag{21}$$

Similar to DCV, y_i is identical for the ith class and the feature dimension of y_i is $c - 1$. With respect to any testing sample $\Phi(x_{test})$, we get its transformed feature vector $y_{test} = W^{\mathrm{T}}\Phi(x_{test})$ to conduct the recognition test. This completes the discriminative feature extraction procedure.

3.3. Biometric recognition procedure using KDCV–RBF classifier

Being a feed-forward neural network, the RBF network has been widely applied to function approximation and pattern recognition. Fig. 4 shows a basic RBF network structure [32].

Generally, the RBF network contains three layers: an input layer, a hidden layer and an output layer. The unit number of the input layer is decided by the feature vector dimension of samples. The units of the hidden layer correspond to the clustering centers of the training sample set. The position and number of units in the hidden layer are adjustable. The unit number of the output layer is equal to the number of classes. For expected output values of all training samples of the ith class, we assign the output value of the ith unit to be 1 and the output values of the other units to be 0. The weights between the input and hidden layers are set as 1, while the weights between the hidden and output layers are adjustable.

Here, we combine the KDCV and RBF network to classify the pixel level fused images. In other words, we present a KDCV–RBF classifier. We employ the same kernel function for both KDCV and RBF network, i.e. the Gaussian function. Following is the whole fusion recognition procedure using the proposed classifier:

Step 1: Pixel level fusion: For the face and palmprint image sample sets X_{face} and X_{palm}, we use the pixel level fusion approach described in Section 2 to get a fused image sample set $X_{norm\text{-}fuse}$. We take the form of feature vector to represent $X_{norm\text{-}fuse}$ and obtain a one-dimensional sample set X.

Step 2: Discriminative feature extraction: For X, we use the KDCV approach to achieve the optimal projection transform W and c nonlinear DCV, which construct the training sample set Y_{train}. Performing W on all testing samples, we get the testing sample set Y_{test}. With respect to the Gaussian kernel function $k(x_1, x_2) = \exp(-\|x_1 - x_2\|^2/2\delta^2)$, δ^2 is set as the variance of the training sample set of X.

Step 3: Classification: Separately input Y_{train} and Y_{test} to the RBF network. The numbers of units in the input, hidden and output layers are $c-1$, c and c, respectively. We use all c nonlinear DCV as the clustering centers, i.e. the hidden units. The unit values of three layers are initially normalized to the range $[-1, 1]$. With respect to the Gaussian radial basis function $g(y_1, y_2) = \exp(-\|y_1 - y_2\|^2/2\delta^2)$, where δ^2 is set as 10 which is slightly better than other values in the experiments. Since the weights between the input and hidden layers are equal to 1, we only need to calculate the weights' matrix W_{RBF} between the hidden and output layers. For Y_{train}, G expresses the hidden layer values, $W_{RBF}G$ denotes the actual output values, and T expresses the expected output values. W_{RBF} is thus computed by

$$W_{RBF} = G^{+}T, \tag{22}$$

where G^{+} is the pseudoinverse of G. Then, we can use the trained RBF network to test the sample set Y_{test}.

Fig. 5 shows the whole recognition procedure.

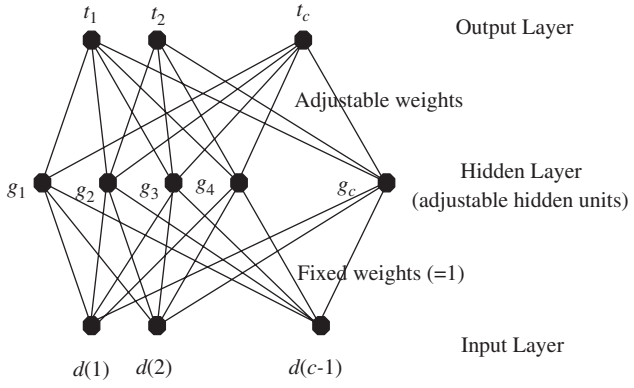

Fig. 4. A basic RBF network structure.

4. Experimental results

In this section, we first introduce two face databases (AR and FERET) and a palmprint database. We then provide biometric fusion results by using two pairs of databases, that is, AR and palmprint databases, and FERET and palmprint databases. The experiments compare pixel level and classifier recognition methods as follows:

Pixel level methods: Use different image data and classify them with the KDCV–RBF classifier (here abbreviated to KDRC). The pixel level methods include: (1) using single-mode original images, respectively, from the AR, FERET and palmprint databases, we have AR-KDRC, FERET-KDRC and Palm-KDRC. (2) Instead of doing a Gabor transform, directly

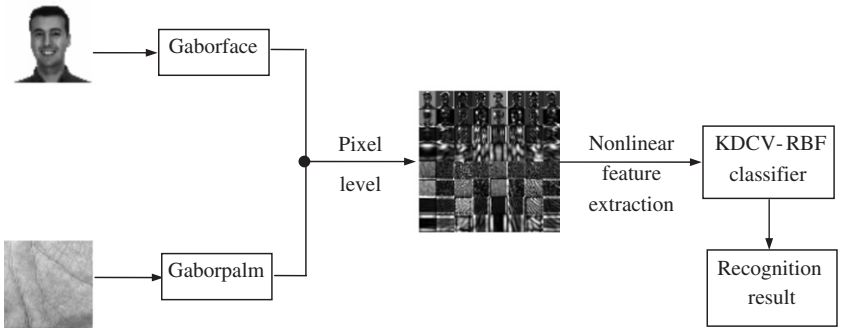

Fig. 5. Multi-modal biometric fusion recognition procedure.

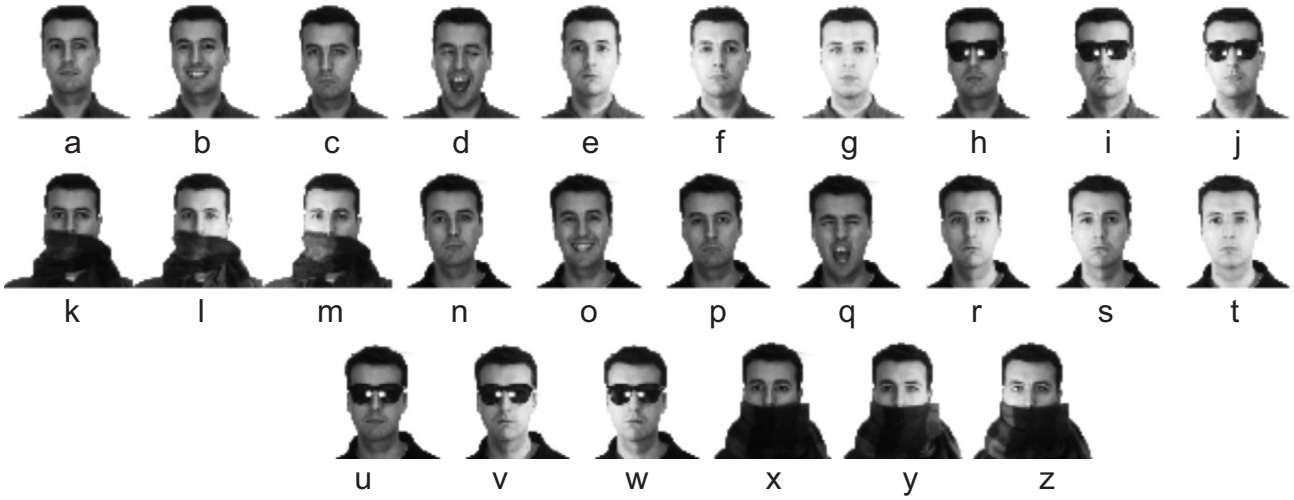

Fig. 6. Demonstration images of one subject from the AR database.

using original images to do pixel level fusion on two pairs of databases (i.e. AR and palmprint, and FERET and palmprint), we have ARPalm-Originalfusion-KDRC and FERETPalm-Originalfusion-KDRC. (3) Doing Gabor transform and pixel level fusion, we have ARPalm-Gaborfusion-KDRC and FERETPalm-Gaborfusion-KDRC.

Classifier methods: Use the fused Gabor-transformed images and classify them with different feature extraction and classification methods. The classifier methods include: (1) using the KDCV and NN classifier (abbreviated to KDNC) on two pairs of databases, we have ARPalm-Gaborfusion-KDNC and FERETPalm-Gaborfusion-KDNC. (2) Using the DCV and NN classifier (DNC), we have ARPalm-Gaborfusion-DNC and FERETPalm-Gaborfusion-DNC. (3) Using the Kernel PCA and NN classifier (KPNC), we have ARPalm-Gaborfusion-KPNC and FERETPalm-Gaborfusion-KPNC. (4) Using the KDRC classifier, we have ARPalm-Gaborfusion-KDRC and FERETPalm-Gaborfusion-KDRC (which are introduced in the last paragraph).

As in the DCV algorithm [28], we employ the Euclidean distance in the NN classification. For the Kernel PCA (KPCA) [26] method, we also use the Gaussian kernel function and take the same parameter setting as KDCV. We do not compare the Kernel LDA method [27] in this paper because, for the small sample recognition problem, KPCA outperforms Kernel LDA in the experiments.

4.1. Introduction of databases

4.1.1. AR face database

The AR face database contains over 4000 color face images of 126 people (70 men and 56 women), including frontal views of faces with different facial expressions, under different lighting conditions and with various occlusions [37]. Most of the pictures were taken in two sessions (separated by two weeks). Each session yielded 13 color images, with 119 individuals (65 men and 54 women) participating in each session. The images of these 119 individuals were selected and used in our experiment for a total number of 3094 ($=119 \times 26$) samples. All color images are transformed into gray images. Each image is 768×576 with 256 gray levels. Each image is scaled to 60×60. Fig. 6 shows all samples of one subject, where (a)–(m) are from Session 1 and (n)–(z) are from Session 2. The details of the images are: (a) and (n), neutral expression; (b) and (o), smile; (c) and (p), anger; (d) and (q), scream; (e) and (r), left light on; (f) and (s), right light on; (g) and (t), all sides light on; (h) and (u), wearing sun glasses; (i) and (v), wearing sun glasses and left light on; (j) and (w), wearing sun glasses and right light on; (k) and (x), wearing scarf; (l) and (y) wearing scarf and left light on; and (m) and (z), wearing scarf and right light on.

4.1.2. FERET face database

The FERET database employed in our experiment includes 2200 facial images corresponding to 200 individuals with each person contributing 11 images [38]. The images are named with two-character strings from ranging "ba" to "bk". The images in this database were captured under various illuminations and display a variety of facial expressions and poses. Each image is 384×256 with 256 gray levels. Since many images in this database include the background and the body chest region, we automatically cropped every image sample. That is, we intercepted a part having the rows from the 40th to the 340th in the original image, producing a part size of 300×256. We performed a histogram equalization on the intercepted images and scaled them to 60×60. Fig. 7 shows all samples of one subject. The details of the images are as follows: (a) regular facial status; (b) $+15^\circ$ pose angle; (c) -15° pose angle; (d) $+40^\circ$ pose angle; (e) -40° pose angle; (f) $+25^\circ$ pose angle; (g) -25° pose angle; (h) alternative expression; (i) different illumination; (j) $+60^\circ$ pose angle; and (k) -60° pose angle.

Fig. 7. Demonstration images of one subject from the FERET database.

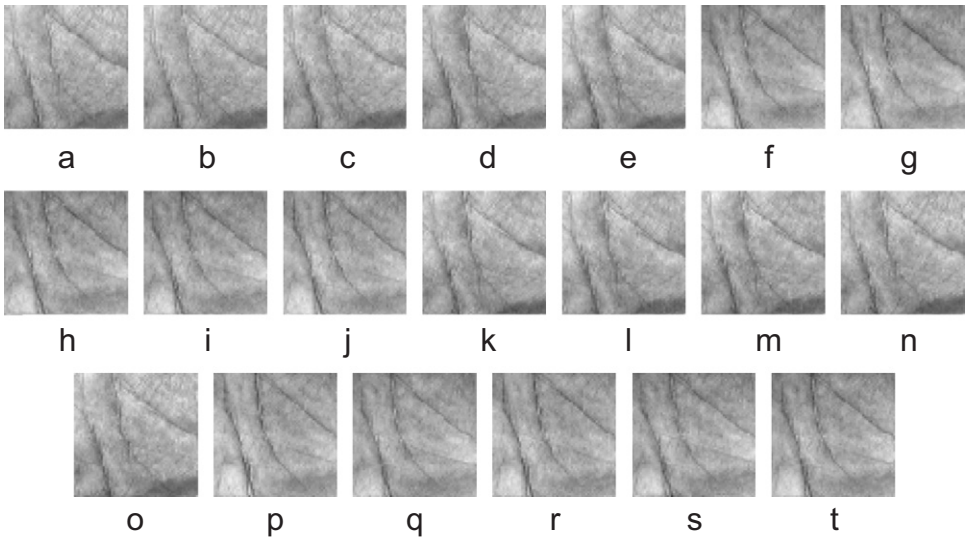

Fig. 8. Demonstration images of one subject from the palmprint database.

4.1.3. Palmprint database

We use a palmprint database provided by the Hong Kong Polytechnic University (HK-PolyU). This database contains palmprint images from 189 individuals. The subjects mainly consist of volunteers from among students and staff at HK-PolyU. The subject was asked to provide about 10 images each of the left palm and the right palm. Each person thus provided 20 images making a database containing a total of 3780 ($=189 \times 20$) images. The size of every original image is 384×284 pixels with 75 dpi resolution. Using the image processing method in [17], the subimages of palmprint part with a fixed size 128×128 were extracted from the original images. In order to reduce the computational cost, each subimage was compressed to 60×60. We took these subimages as palmprint image samples for our experiments. Fig. 8 shows all the samples from one subject. The major changes are in illumination, position including shift and rotation, and texture details. Similar to the kinds of changes encountered in facial expressions, the image may also be slightly affected by the way the hand is posed, shrunk, or stretched.

4.2. Biometric recognition using AR face database and palmprint database

The AR face database has 119 classes with each class containing 26 samples. The palmprint database contains 189 classes with each class containing 20 samples. We take sample subsets of the same size from these two databases. In other words, we use all 119 face classes with each class containing the first 20 samples, and use the first 119 palmprint classes with each class containing all 20 samples. For small sample biometric recognition, we set the numbers of training samples per class to be 2 and 3, respectively, and the remainder are used as testing samples.

Firstly, we set the number of training samples per class to be 2 so that there are 238 ($=119 \times 2$) training samples and 2142 ($=119 \times 18$) testing samples. Fig. 9(a) shows the results of 30 random tests of AR-KDRC, Palm-KDRC, ARPalm-Originalfusion-KDRC and ARPalm-Gaborfusion-KDRC. It can be seen that the pixel level fusion methods clearly improve the recognition performance of AR-KDRC and

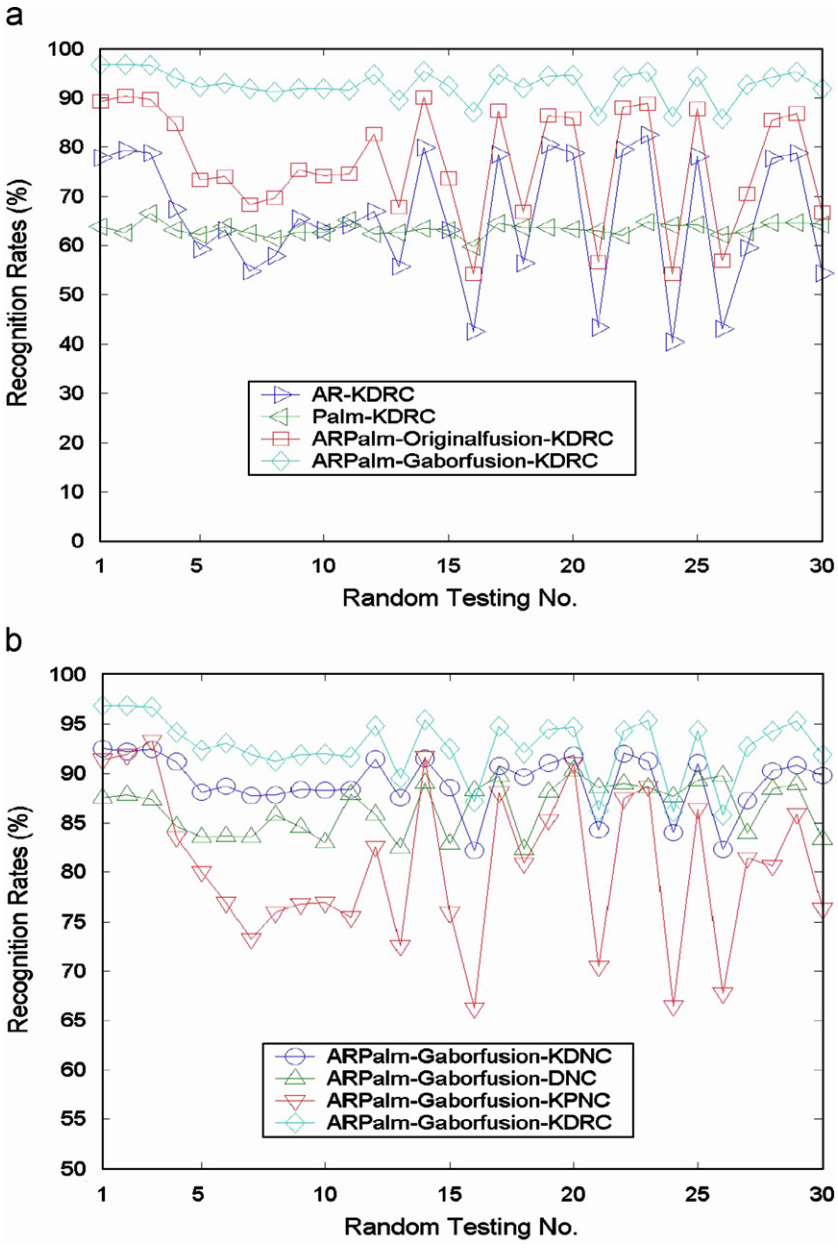

Fig. 9. Random testing results using AR and palmprint databases where the number of training samples per class is 2.

Palm-KDRC, and ARPalm-Gaborfusion-KDRC performs better than others in all cases. Fig. 9(b) shows the random testing results of ARPalm-Gaborfusion-KDNC, ARPalm-Gaborfusion-DNC, ARPalm-Gaborfusion-KPNC and ARPalm-Gaborfusion-KDRC. In most cases, ARPalm-Gaborfusion-KDNC outperforms ARPalm-Gaborfusion-DNC and ARPalm-Gaborfusion-KPNC. And, ARPalm-Gaborfusion-KDRC achieves better recognition results than ARPalm-Gaborfusion-KDNC.

Secondly, we set the number of training samples per class to be 3 so that there are 357 ($=119 \times 3$) training samples and 2023 ($=119 \times 17$) testing samples. Fig. 10 (a) shows the results of 30 random tests of AR-KDRC, Palm-KDRC, ARPalm-Originalfusion-KDRC and ARPalm-Gaborfusion-KDRC. It shows that ARPalm-Gaborfusion-KDRC gets the best results in all cases. Fig. 10(b) shows the random testing results of ARPalm-Gaborfusion-KDNC, ARPalm-Gaborfusion-DNC, ARPalm-Gaborfusion-KPNC and ARPalm-Gaborfusion-KDRC. In almost all cases, ARPalm-Gaborfusion-KDRC performs best.

Table 2 shows the average recognition results for all the methods that are compared. AR-KDRC and Palm-KDRC are single-mode biometric methods. They achieve total average recognition rates of 71.28% and 63.81%, respectively. Performing the Gabor-based pixel level fusion (ARPalm-Gaborfusion-KDRC) improves the total rate to 94.40%. Table 2 also shows that KDCV is an effective feature extraction approach, performing better than DCV and KPCA, and that the RBF network is more suitable for classifying the KDCV features than the NN

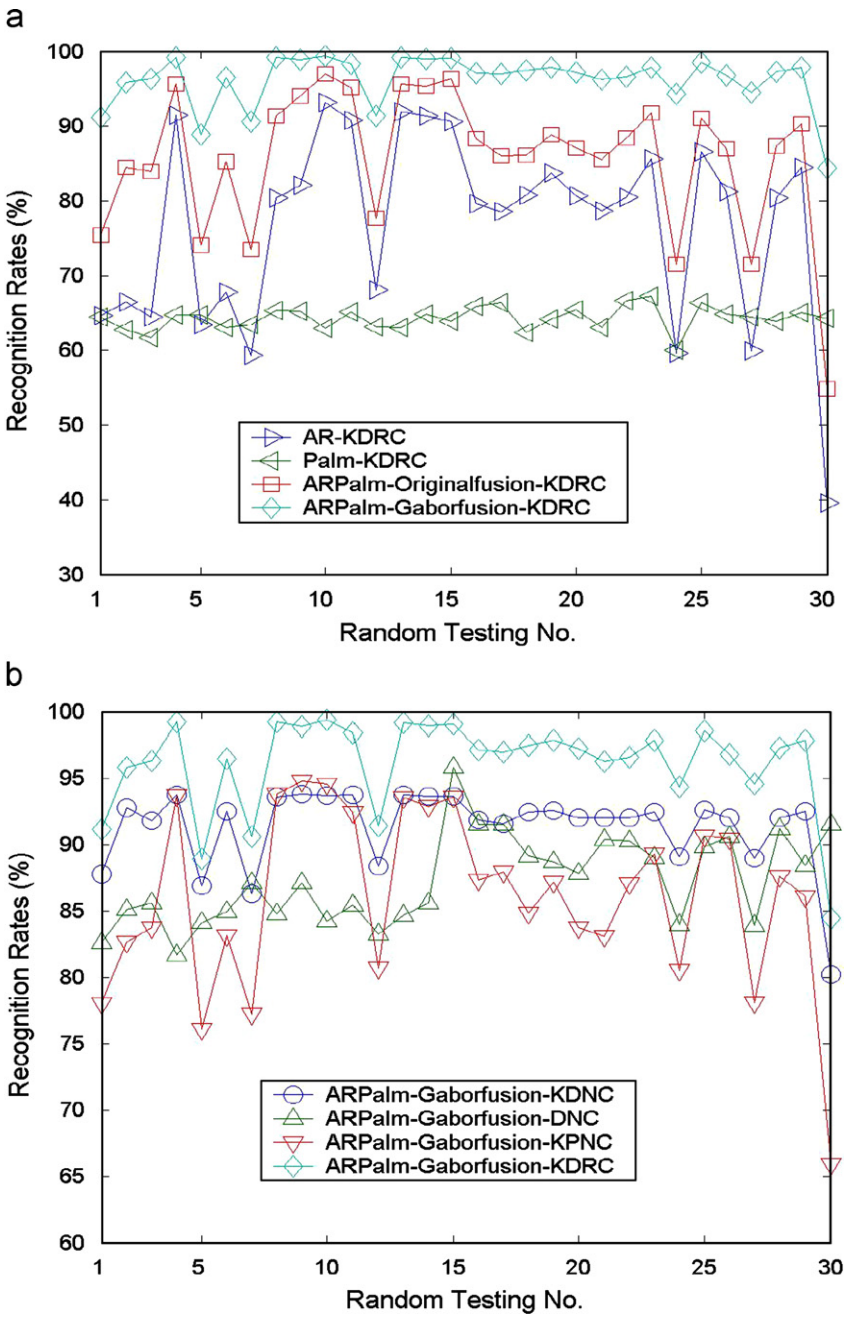

Fig. 10. Random testing results using AR and palmprint databases where the number of training samples per class is 3.

Table 2
Average recognition results using AR and palmprint databases

Methods	Recognition rates (%)		
	Number of training samples per class		Total mean values
	2	3	
	Mean values and variances	Mean values and variances	
AR-KDRC	65.67 ± 13.16	76.88 ± 12.80	71.28
Palm-KDRC	63.33 ± 1.30	64.29 ± 1.57	63.81
ARPalm-Originalfusion-KDRC	76.67 ± 11.68	85.70 ± 9.57	81.19
ARPalm-Gaborfusion-KDNC	89.12 ± 2.87	91.35 ± 3.00	90.24
ARPalm-Gaborfusion-DNC	86.54 ± 2.61	87.33 ± 3.39	86.94
ARPalm-Gaborfusion-KPNC	80.70 ± 7.94	86.02 ± 6.79	83.36
ARPalm-Gaborfusion-KDRC	92.66 ± 3.08	96.14 ± 3.53	94.40

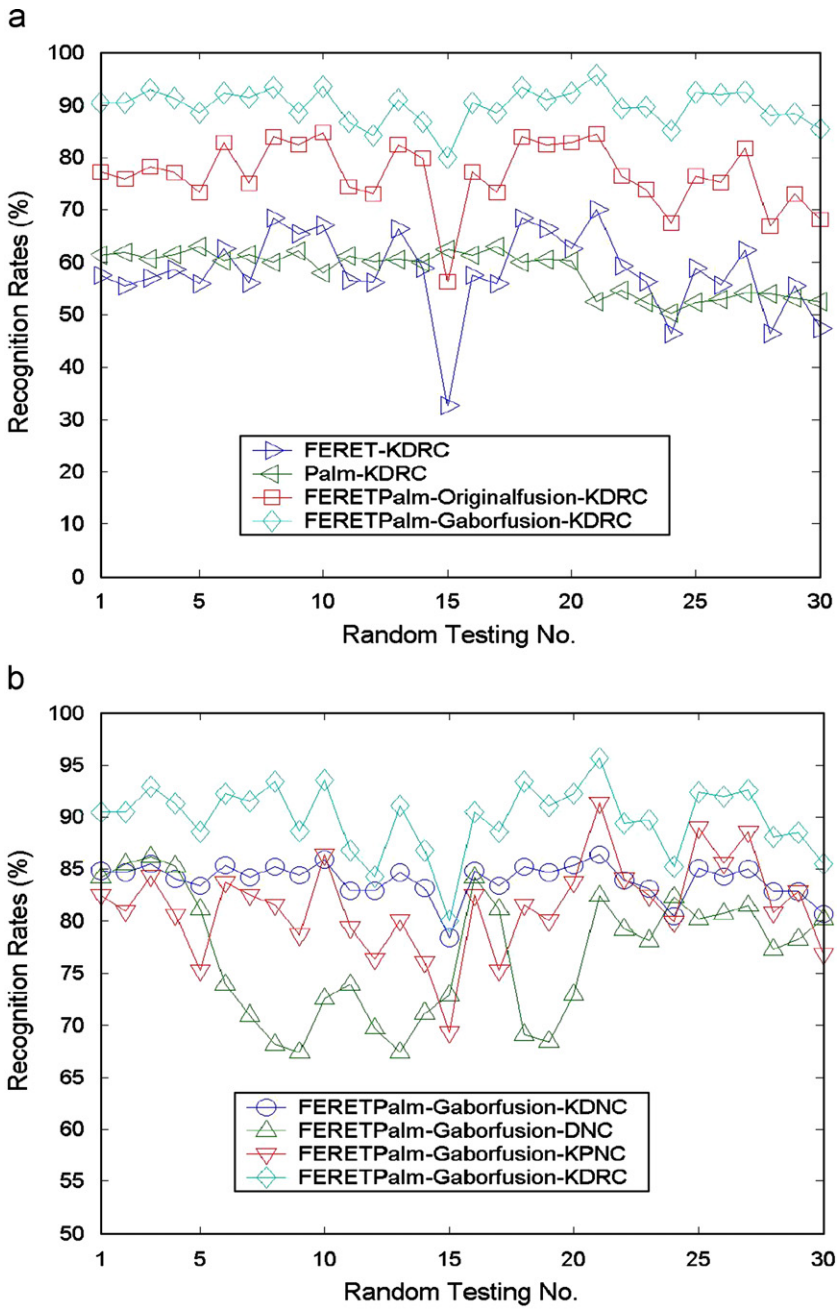

Fig. 11. Random testing results using FERET and palmprint databases where the number of training samples per class is 2.

method. The total average recognition rates of the KDRC classifier is significantly better than that of both the DNC classifier at 7.46% (=94.40% − 86.94%) and the KPNC classifier at 11.04% (=94.40% − 83.36%).

4.3. Biometric recognition using FERET face database and palmprint database

The FERET face database contains 200 classes with each class containing 11 samples. The palmprint database contains 189 classes with each class containing 20 samples. To implement the biometric fusion, we take sample subsets of the same size from these two databases. That is, we use the first 189 face classes with each class containing all 11 samples, and use all 189 palmprint classes with each class containing the first 11 samples. For small sample biometric recognition, we set the numbers of training samples per class to be 2 and 3, respectively, and the remainder are used as testing samples.

We first set the number of training samples per class at 2. The number of training and testing samples is thus, respectively, 378 (=189 × 2) and 1701 (=189 × 9). Fig. 11(a) shows the results of 30 random tests of FERET-KDRC, Palm-KDRC, FERETPalm-Originalfusion-KDRC and FERETPalm-Gaborfusion-KDRC. Pixel level fusion methods are

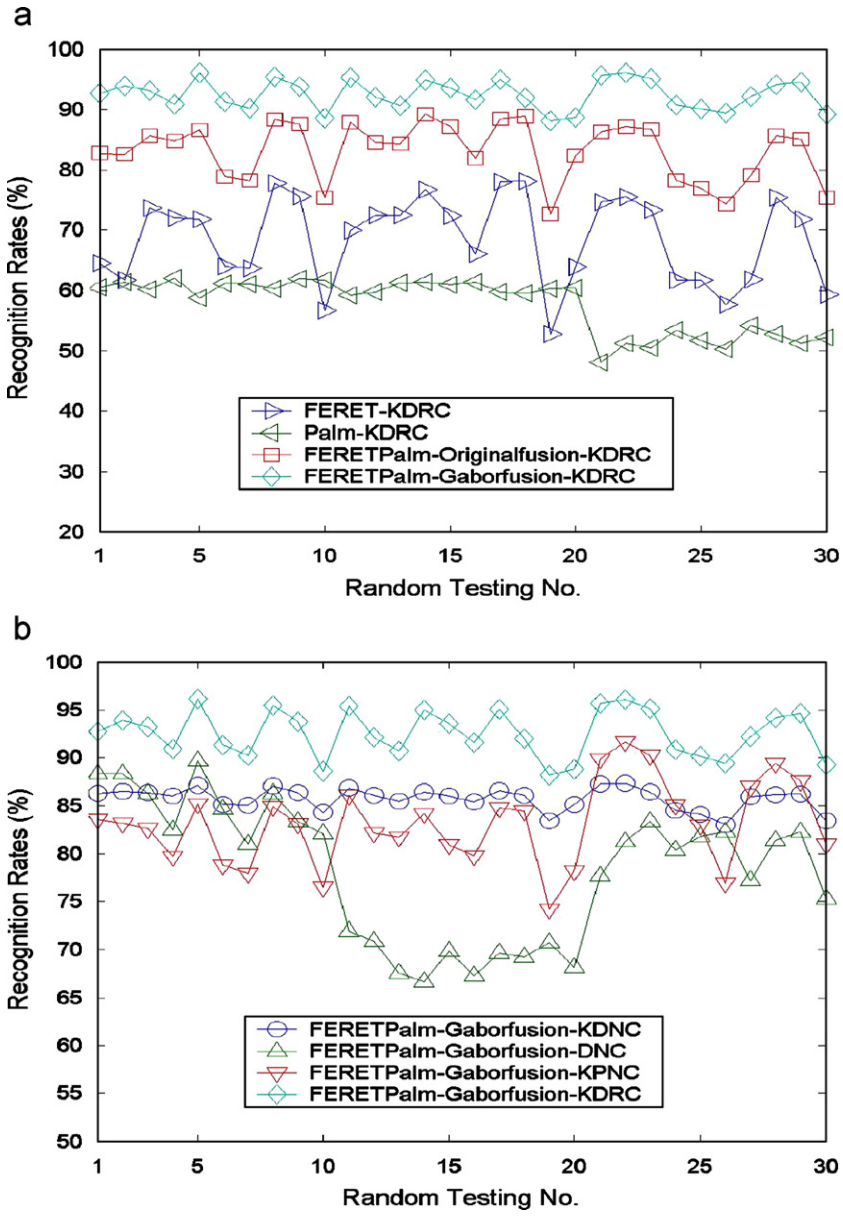

Fig. 12. Random testing results using FERET and palmprint databases where the number of training samples per class is 3.

obviously superior to single-mode biometric methods, and in all cases FERETPalm-Gaborfusion-KDRC performs better than FERETPalm-Originalfusion-KDRC. Fig. 11(b) shows the random testing results of FERETPalm-Gaborfusion-KDNC, FERETPalm-Gaborfusion-DNC, FERETPalm-Gaborfusion-KPNC and FERETPalm-Gaborfusion-KDRC. In most cases, FERETPalm-Gaborfusion-KDNC outperforms FERETPalm-Gaborfusion-DNC and FERETPalm-Gaborfusion-KPNC. In all cases, FERETPalm-Gaborfusion-KDRC achieves better recognition results than FERETPalm-Gaborfusion-KDNC.

Second, we set the number of training samples per class to be 3. The number of training and testing samples is thus, respectively, 567 (=189 × 3) and 1512 (=189 × 8). Fig. 12(a) shows the results of 30 random tests of FERET-KDRC, Palm-KDRC, FERETPalm-Originalfusion-KDRC and FERETPalm-Gaborfusion-KDRC. It shows that the pixel level fusion methods outperform FERET-KDRC and Palm-KDRC in all cases, and FERETPalm-Gaborfusion-KDRC obtains best recognition results. Fig. 12(b) shows the random testing results of FERETPalm-Gaborfusion-KDNC, FERETPalm-Gaborfusion-DNC, FERETPalm-Gaborfusion-KPNC and FERETPalm-Gaborfusion-KDRC. In all cases, FERETPalm-Gaborfusion-KDRC performs best.

Table 3 shows the average recognition results of all the methods that are compared. FERET-KDRC and Palm-KDRC are single-mode biometric methods. They achieve total average recognition rates of 63.35% and 57.95%, respectively. Performing the Gabor-based pixel level fusion (FERETPalm-Gaborfusion-KDRC) improves the total rate to 91.22%. Table 3 also shows that KDCV outperforms DCV and KPCA, and the RBF network is more suitable for classifying the KDCV features than the NN method. The total average recognition rate of

Table 3
Average recognition results using FERET and palmprint databases

Methods	Recognition rates (%)		
	Number of training samples per class		Total mean values
	2	3	
	Mean values and variances	Mean values and variances	
FERET-KDRC	58.11 ± 7.79	68.58 ± 7.19	63.35
Palm-KDRC	58.25 ± 4.06	57.65 ± 4.54	57.95
FERETPalm-Originalfusion-KDRC	76.70 ± 6.40	83.11 ± 4.89	79.91
FERETPalm-Gaborfusion-KDNC	83.93 ± 1.72	85.77 ± 1.17	84.85
FERETPalm-Gaborfusion-DNC	76.89 ± 6.09	78.26 ± 7.24	77.58
FERETPalm-Gaborfusion-KPNC	81.40 ± 4.55	83.14 ± 4.30	82.27
FERETPalm-Gaborfusion-KDRC	89.90 ± 3.32	92.53 ± 2.46	91.22

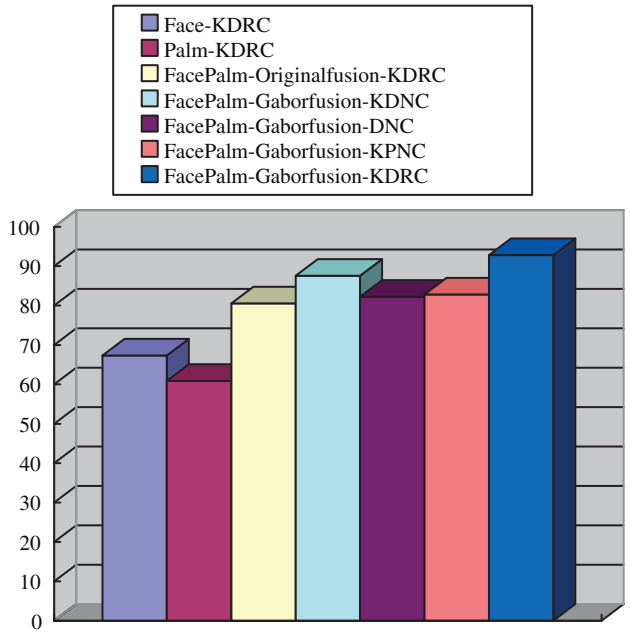

Fig. 13. Total average recognition rates of face and palmprint biometric recognition.

the KDRC classifier is significantly better than that of both the DNC and KPNC classifiers at 13.64% (=91.22% − 77.58%) and 8.95% (=91.22% − 82.27%), respectively.

4.4. Analysis of experimental results

Based on Tables 2 and 3, Fig. 13 shows the total average recognition rates for the two groups of experiments in Sections 4.2 and 4.3. From Fig. 13, the total recognition rates are raised from 67.32% (face recognition) and 60.88% (palmprint recognition) to 92.81% (multi-modal fusion biometric). By performing the Gabor transform, FacePalm-Gaborfusion-KDRC is 12.26% better than FacePalm-Originalfusion-KDRC, which uses the original biometric images. Further, the proposed KDRC classifier improves the total recognition rates of two representative classifiers (DNC and KPNC) by 10.55% and 9.99%.

We evaluate these experimental results using the null hypothesis statistical test based on the Bernoulli model [39,40]. If the resulting p-value is below the desired significance level (i.e. 0.01), the null hypothesis is rejected and the performance difference between two algorithms are considered statistically significant. Table 4 analyzes the statistical difference in the recognition performance of the proposed FacePalm-Gaborfusion-KDRC approach and a compared method FacePalm-Gaborfusion-KDNC. In Table 4, the item "Number of significant differences ($p < 0.01$)" means the number of statistically significant differences between two compared methods at a significance level of "$p < 0.01$" in the trials. In most trials, there are significant differences between FacePalm-Gaborfusion-KDRC and FacePalm-Gaborfusion-KDNC.

Table 5 shows the total statistical difference analysis for FacePalm-Gaborfusion-KDRC and other compared methods. The item "Number of significant differences ($p < 0.01$) for random test (60 times)" contains 60 random tests while the number of training samples per class ranges from 2 to 3. Table 5 shows that the proposed new approach makes a significant difference to the recognition performance in comparison with the other methods.

5. Conclusion

In the field of biometric feature recognition, multi-modal biometric fusion techniques are now attracting increasing attention and interest among researchers. The small sample recognition problem is a research difficulty of biometric because this problem often leads to unsatisfactory recognition performance in real-world applications. In this paper, we present a pixel level biometric fusion approach to solve this problem. We first combine the normalized Gabor-transformed face and palmprint images at the pixel level. We then present a novel classifier, KDCV-RBF (KDRC), to classify the fused biometric images. The proposed classifier uses a new nonlinear discriminative feature extraction approach, the KDCV approach, and the RBF classification method. As the test data, we use two large face databases (AR and FERET) and a large palmprint database as the test data. The experimental results demonstrate

Table 4
Statistical difference analysis between two methods

Two compared methods	Employed databases	Number of training samples per class	Statistical difference analysis	
			Random test (30 times)	Number of significant differences ($p < 0.01$)
FacePalm-Gaborfusion-KDRC and FacePalm-Gaborfusion-KDNC	AR and Palmprint	2	0, 0, 0, 1e − 9, 3e − 8, 4e − 8, 2e − 7, 1e − 5, 8e − 6, 6e − 6, 2e − 5, 1e − 13, 0.0102, 0, 7e − 7, 7e − 8, 5e − 25, 1e − 4, 1e − 15, 8e − 10, 0.0221, 2e − 6, 1e − 16, 0.0169, 4e − 13, 6e − 5, 1e − 35, 3e − 17, 0, 0.0025	27
		3	4e − 7, 2e − 6, 1e − 13, 6e − 25, 0.0048, 2e − 10, 4e − 11, 2e − 28, 2e − 20, 1e − 26, 6e − 16, 1e − 5, 3e − 24, 3e − 23, 1e − 23, 1e − 18, 8e − 20, 3e − 18, 2e − 19, 5e − 20, 4e − 11, 1e − 13, 1e − 21, 3e − 17, 1e − 26, 3e − 16, 3e − 19, 1e − 19, 8e − 22, 1e − 7	30
	FERET and Palmprint	2	6e−9, 7e−10, 2e−15, 1e−14, 1e−7, 6e − 14, 2e − 15, 3e − 19, 1e − 5, 6e − 18, 6e − 5, 0.1075, 2e − 11, 2e−4, 0.0771, 6e−9, 1e−7, 3e−19, 2e − 11, 6e − 14, 3e − 27, 2e − 8, 4e − 12, 1e − 6, 2e − 14, 3e − 17, 1e − 15, 8e − 8, 1e − 8, 2e − 6	28
		3	4e−9, 4e−12, 2e−10, 1e−5, 2e−18, 2e − 8, 3e − 6, 2e − 15, 1e − 11, 1e−4, 3e−17, 2e−8, 2e−6, 4e−16, 1e − 12, 1e − 8, 2e − 16, 7e − 8, 2e−5, 3e−4, 3e−16, 1e−17, 1e−16, 1e−8, 4e−8, 6e−9, 2e−8, 1e−13, 2e − 15, 6e − 8	30

Table 5
Analysis of total statistical difference

FacePalm-Gaborfusion-KDRC and other compared methods	Employed databases	Statistical difference analysis	
		Number of significant differences ($p < 0.01$) for random test (60 times)	Average number
Face-KDRC	AR and Palmprint	60	60
	FERET and Palmprint	60	
Palm-KDRC	AR and Palmprint	60	60
	FERET and Palmprint	60	
FacePalm-Originalfusion-KDRC	AR and Palmprint	60	60
	FERET and Palmprint	60	
FacePalm-Gaborfusion-KDNC	AR and Palmprint	57	57.5
	FERET and Palmprint	58	
FacePalm-Gaborfusion-DNC	AR and Palmprint	55	57
	FERET and Palmprint	59	
FacePalm-Gaborfusion-KPNC	AR and Palmprint	60	60
	FERET and Palmprint	60	

that the proposed novel approach is an effective solution for the small sample biometric recognition problem.

Acknowledgment

The work described in this paper is fully supported by the National Natural Science Foundation of China (NSFC) under Project No. 60402018, Project No. 60632050, Project No. 60472060, and Project No. 60332010.

References

[1] D. Zhang, X. Jing, J. Yang, Biometric Images Discrimination (BID) Technologies, IGP/INFOSCI/IRM Press, 2006, ISBN 1-59140-831-8.
[2] D. Zhang, A.K. Jain, Proceedings of the First International Conference on Biometric Authentication (ICBA), Lecture Notes in Computer Science, vol. 3072, Springer, Berlin, 2004.
[3] D. Zhang, Biometrics Solutions for Authentication in an e-World, Kluwer Academic Publishers, Dordrecht, 2002, ISBN 1-4020-7142-6.
[4] L. Chen, H.M. Liao, M. Ko, J. Lin, G. Yu, A new LDA-based face recognition system which can solve the small sample size problem, Pattern Recognition 33 (10) (2000) 1713–1726.
[5] X.Y. Jing, D. Zhang, Y.F. Yao, Improvements on the linear discrimination technique with application to face recognition, Pattern Recognition Lett. 24 (15) (2003) 2695–2701.
[6] X.Y. Jing, D. Zhang, Y.Y. Tang, An improved LDA approach, IEEE Trans. Syst. Man Cybern. Part B 34 (5) (2004) 1942–1951.
[7] L. Hong, A.K. Jain, Integrating faces and fingerprints for personal identification, IEEE Trans. Pattern Anal. Mach. Intell. 20 (12) (1998) 1295–1307.
[8] A.K. Jain, A. Ross, Learning user-specific parameters in a multibiometric system, Proceedings of ICIP 2002, New York, 2002, pp. 57–70.
[9] A. Ross, A.K. Jain, Information fusion in biometrics, Pattern Recognition Lett. 24 (13) (2003) 2115–2125.
[10] V. Chatzis, A.G. Bors, I. Pitas, Multimodal decision-level fusion for person authentication, IEEE Trans. Syst. Man Cybern. Part A 29 (6) (1999) 674–680.
[11] P. Verlinde, G. Chollet, M. Acheroy, Multi-modal identity verification using expert fusion, Inf. Fusion 1 (1) (2000) 17–33.
[12] S. Prabhakar, A.K. Jain, Decision-level fusion in fingerprint verification, Pattern Recognition 35 (4) (2002) 861–874.
[13] J. Kittler, M. Hatef, R.P.W. Duin, J. Matas, On combining classifiers, IEEE Trans. Pattern Anal. Mach. Intell. 20 (3) (1998) 226–239.
[14] L. Wang, T. Tan, W. Hu, H. Ning, Automatic gait recognition based on statistical shape analysis, IEEE Trans. Image Process. 12 (9) (2003) 1120–1131.
[15] K. Chang, K. Bowyer, V. Barnabas, Comparison and combination of ear and face images in appearance-based biometrics, IEEE Trans. Pattern Anal. Mach. Intell. 25 (9) (2003) 1160–1165.
[16] J. Daugman, How iris recognition works, IEEE Trans. Circuits Syst. Video Technol. 14 (1) (2004) 21–30.
[17] D. Zhang, W.K. Kong, J. You, M. Wong, On-line palmprint identification, IEEE Trans. Pattern Anal. Mach. Intell. 25 (9) (2003) 1041–1050.
[18] O. Ayinde, Y.H. Yang, Face recognition approach based on rank correlation of Gabor-filtered images, Pattern Recognition 35 (6) (2002) 1275–1289.
[19] C. Liu, H. Wechsler, Gabor feature based classification using the enhanced Fisher linear discriminant model for face recognition, IEEE Trans. Image Process. 11 (4) (2002) 467–476.
[20] W.K. Kong, D. Zhang, W. Li, Palmprint feature extraction using 2-D Gabor filters, Pattern Recognition 36 (10) (2003) 2339–2347.
[21] R. Chellappa, C.L. Wilson, S. Sirohey, Human and machine recognition of faces: a survey, Proc. IEEE 83 (5) (1995) 705–740.
[22] M. Turk, A. Pentland, Eigenfaces for recognition, Int. J. Cognitive Neurosci. 3 (1) (1991) 71–86.
[23] P.N. Belhumeur, J.P. Hespanha, D.J. Kriegman, Eigenfaces vs. fisherface: recognition using class specific linear projection, IEEE Trans. Pattern Anal. Mach. Intell. 19 (7) (1997) 711–720.
[24] H. Yu, J. Yang, A direct LDA algorithm for high-dimensional data with application to face recognition, Pattern Recognition 34 (12) (2001) 2067–2070.
[25] X.Y. Jing, D. Zhang, Z. Jin, UODV: improved algorithm and generalized theory, Pattern Recognition 36 (11) (2003) 2593–2602.
[26] B. Scholkopf, A. Smola, K. Muller, Nonlinear component analysis as a Kernel eigenvalue problem, Neural Comput. 10 (5) (1998) 1299–1319.
[27] G. Baudat, F. Anouar, Generalized discriminant analysis using a Kernel approach, Neural Comput. 12 (10) (2000) 2385–2404.
[28] H. Cevikalp, M. Neamtu, M. Wilkes, A. Barkana, Discriminative common vectors for face recognition, IEEE Trans. Pattern Anal. Mach. Intell. 27 (1) (2005) 4–13.
[29] W. Pedrycz, Conditional fuzzy clustering in the design of radial basis function neural networks, IEEE Trans. Neural Networks 9 (4) (1998) 601–612.
[30] A. Esposito, M. Marinaro, D. Oricchio, S. Scarpetta, Approximation of continuous and discontinuous mappings by a growing neural RBF-based algorithm, Neural Networks 13 (6) (2000) 651–665.
[31] K.Z. Mao, RBF neural network center selection based on Fisher ratio class separability measure, IEEE Trans. Neural Networks 13 (5) (2002) 1211–1217.
[32] M.J. Er, S.Q. Wu, J.W. Lu, H.L. Toh, Face recognition with radial basis function (RBF) neural networks, IEEE Trans. Neural Networks 13 (3) (2002) 697–710.
[33] F. Girosi, T. Poggio, Networks and the best approximation property, Biol. Cybern. 63 (3) (1990) 169–176.
[34] S. Haykin, Neural Networks: A Comprehensive Foundation, second ed., Prentice-Hall, Englewood Cliffs, NJ, 1999, ISBN: 0-13-273350-1.
[35] M.B. Gulmezoglu, V. Dzhafarov, A. Barkana, The common vector approach and its relation to principal component analysis, IEEE Trans. Speech Audio Process. 9 (6) (2001) 655–662.
[36] Z.Z. Liang, P.F. Shi, Uncorrelated discriminant vectors using a kernel method, Pattern Recognition 38 (2) (2005) 307–310.
[37] A.M. Martinez, R. Benavente, The AR face database, CVC Technical Report, no. 24, June 1998.
[38] P.J. Phillips, H. Wechsler, J. Huang, P. Rauss, The FERET database and evaluation procedure for face-recognition algorithms, Image Vision Comput. 16 (5) (1998) 295–306.
[39] W. Yambor, B. Draper, R. Beveridge, Analyzing PCA-based face recognition algorithms: eigenvector selection and distance measures, in: H. Christensen, J. Phillips (Eds.), Empirical Evaluation Methods in Computer Vision, World Scientific Press, Singapore, 2002.
[40] J.R. Beveridge, K. She, B. Draper, G.H. Givens, Parametric and nonparametric methods for the statistical evaluation of human ID algorithms, Proceedings of the Third Workshop Empirical Evaluation of Computer Vision Systems, 2001.
[41] X.Y. Jing, D. Zhang, Z. Jin, Improvements on the uncorrelated optimal discriminant theory, Pattern Recognition 36 (8) (2003) 1921–1923.
[42] X.Y. Jing, H. Wong, D. Zhang, Face recognition based on discriminant fractional Fourier feature extraction, Pattern Recognition Lett. 27 (13) (2006) 1465–1471.
[43] X.Y. Jing, D. Zhang, A face and palmprint recognition approach based on discriminant DCT feature extraction, IEEE Trans. Systems Man Cybernet. B 34 (6) (2004) 2405–2415.

About the Author—XIAO-YUAN JING received his M.Sc. and Ph.D. in Pattern Recognition from Nanjing University of Science and Technology (1995 and 1998, respectively), China. He is now a Professor and Doctor Supervisor at the Nanjing University of Posts and Telecommunications, China. He was a visiting scholar at the Hong Kong Polytechnic University and the Hong Kong Baptist University. His research interest includes biometrics, pattern recognition, image processing, neural networks, machine learning and artificial intelligence.

About the Author—YONG-FANG YAO received her Master degree in Computer Application from the Beijing Institute of Technology in 2007. She ever worked as a computer engineer at two IT corporations. She is now working at the Nanjing University of Posts and Telecommunications, China. Her research interest includes biometrics recognition, image processing and artificial intelligence.

About the Author—DAVID ZHANG received his M.Sc. and Ph.D. in Computer Science from the Harbin Institute of Technology (1982 and 1985, respectively). In 1994, he received his second Ph.D. in Electrical and Computer Engineering from the University of Waterloo, Canada. Currently he is a Chair Professor at the Hong Kong Polytechnic University, where he is the founding director of the Biometrics Technology Center supported by the Hong Kong SAR government. His research interest includes biometrics, image processing and pattern recognition.

About the Author—JING-YU YANG is now a Professor and Doctor Supervisor at the Institute of Computer Science, Nanjing University of Science and Technology, China. He has authored and co-authored more than 200 academic papers. His research interest includes pattern recognition, artificial intelligence, biometrics and robotics.

About the Author—MIAO LI received her Master degree in Computer Science from the Harbin Institute of Technology in 2006. She is now reading for the Ph.D. in Computer Science at the Harbin Institute of Technology, China. Her research interests include image processing and pattern recognition.